Research in Engineering Design (1996) 2: 99–115

Research in
Engineering
Design

Functional Tolerancing: A Design for Manufacturing Methodology

R. S. Srinivasan, K. L. Wood and D. A. McAdams
Department of Mechanical Engineering, The University of Texas, Austin, USA

Abstract. *The problem addressed in this paper is the development of a physico-mathematical basis for mechanical tolerances. The lack of such a basis has fostered a decoupling of design (function) and manufacturing. The groundwork for a tolerancing methodology is laid by a model of profile errors, whose components are justified by physical reasoning and estimated using mathematical tools. The methodology is then presented as an evolutionary procedure that harnesses the various tools, as required, to* analyze *profiles in terms of a minimum set of profile parameters and to* re-generate *them from the parameters. This equips the designer with a rational means for estimating performance prior to manufacturing, hence integrating design and manufacturing. The utility of the* functional tolerancing *methodology is demonstrated with performance simulations of a lathe-head-stock design, focusing on gear transmission with synthesized errors.*

Keywords. Design methodology; Functional tolerancing; Lathe design; Machine precision; Wavelets

1. Perspectives on Tolerances in Design for Manufacturing

Tolerancing is an important issue in the context of modern design. Its evolution is presented as a motivation to the theme of this paper. In this theme, there are two important aspects (among a myriad) of engineering: an idea emanating to satisfy some need, and the physical embodiment of the idea, an artifact. In existent terminology, the former is a component of *design*, and transformation to the latter includes *manufacturing*. The idea results from knowledge of, or intuition about, the physical laws of nature, gained by experience and honed by intellectual introspection. The artifact, on the other hand, results from knowledge of, intuition about, and craftsman skills in fabrication technologies and their applications.

Correspondence and offprint requests to Prof. K. L. Wood, Department of Mechanical Engineering, ETC 4.132, The University of Texas, Austin, TX 78712-1063, USA.

Prior to the industrial revolution, design and manufacturing activities were physically unified, in that an artisan typically designed and also made the artifacts [34]. As the artifacts became more complex, and the users more diverse, a gradual dichotomy of design and manufacturing was inevitable. Today, design and manufacturing are distinct specializations, in stark contrast to their unified genesis. An important ramification of this dichotomy is the need to re-integrate design and manufacturing through information representation and sharing. A critical component of this integration is *tolerance information* [26, 28, 29, 30], linking the precision of manufacturing to the performance (or function) of design concepts.

1.1. The Need for Functional Tolerancing?

Tolerances have important repercussions on several areas of product development, e.g., production, metrology, assembly, and performance; there are several methods that address specific areas in the above list [30]. However, there is no technique that explicitly links tolerance to function [34], i.e., to describe systematically function-driven tolerance assignments, and the means to achieve them [32]. This forms the niche of this research, i.e., the development of a methodology for *functional tolerancing* within the context of design for manufacturing (DFM).

The importance of tolerances is reiterated in the context of design for manufacturing. The paucity of research in functionally-oriented tolerances identifies the problem areas for the paper. In a recent mechanical tolerancing workshop, Tipnis [32] indicates that '... participants could not present any documented case studies as to why specific tolerances were chosen and how these tolerances were achieved ...'. Likewise, in a recent review of engineering design research, it is stated [7], 'Although tolerances are critical to both functional performance and manufacturing cost, tolerances have received very little theoretical treatment ... Research into the effects of tolerances

on functional performance is even more limited.' These statements reveal the need for a basic theory and methods to assess the effect of tolerance scale errors on part performance, the precursor to assigning appropriate tolerances.

In addition to assigning a tolerance by a device function, an understanding of the manufacturability of the tolerance is also essential for a successful design for manufacturing approach. Engineering design is primarily an informational domain, where qualitative customer requirements are transformed through functional prescription, into quantitative, tangible, and (perhaps) non-unique physical descriptions. Geometry is the usual language used for representing such descriptions, including material specifications. These design descriptions are communicated to manufacturing. Manufacturing, a predominantly physical domain, involves the realization of the artifact; in the course of this realization, inherent variabilities in the manufacturing process, or material and tool properties, result in parts with non-ideal geometries and material characteristics. Both these factors play significant roles in determining the mechanical characteristics, and ultimately the functionality of the product. Therefore, the need to exercise control on these deviations requires information feedback of various error sources from manufacturing to design. This information is incorporated in subsequent design specifications. The methodology and tools presented in this paper provide a first step toward monitoring, representating, and incorporating both surface texture and integrity in the processes of both design and manufacture.

1.2. Relating Surface Profile Structures and Design Function

The need for a tolerance that is specified by a desired device function is made clear by examining some of the shortcomings of current tolerancing techniques and error descriptions. In traditional descriptions of manufactured surfaces, the errors are divided into roughness, waviness, and overall form errors. The dividing line between these various components is ill-defined [25]. On a qualitative level, roughness is considered as high frequency variations, and waviness as relatively low frequency variations. Waviness constitutes geometric errors in the tolerance scales. The quantification of these criteria is expressed in terms of *cut-off* values, which are usually determined by instrument or computational limitations [18]. In practice all errors with wavelengths longer than the cut-off are filtered, and the resulting profile is studied. While these are conventional classifications, there is an emerging school of thought that favors a *complete* surface description scheme [18]. In most cases, roughness is considered to be the significant parameter influencing the function of the surface, and waviness is relegated to a secondary status, and even ignored [18, 31]. However, in reality, waviness *is* a significant factor. To illustrate this point, an example from industry, cited in [31], is summarized below.

An automobile manufacturer traced the catastrophic failures in engines to an increase in the surface roughness amplitudes in the crankshaft journals. Corrective procedures were installed in the defective production line to reduce the roughness, and a precautionary polishing process was added. The result was an exponential increase in the number of failures! A complete profile analysis revealed significant waviness in the journal, which reduced normal contact area between the journal and the bearing. The polishing process reduced the contact area further, leading to the increased failures. The waviness was finally attributed to a defective bearing in a machine tool.

This, and similar practical examples, reinforce the trend towards a complete characterization, as opposed to imposing an arbitrary cut-off. A full surface characterization would also be more logical from a manufacturing standpoint. In the course of machining a part, the machining system is subjected to a number of error sources. Each of these error sources conceivably possesses a different natural frequency, and wavelength, and the surface profile is the result of the extremely complex interaction between these errors. Hence it is more rational, and more general, to assess the (complete) profile impartially, as opposed to being prejudiced about short or long wavelengths.

Although this paper does not address all of the issues necessary for a complete description of geometric tolerance, several significant contributions are made toward such a goal. A new superposition approach, incorporating a novel fractal and wavelet representation, is used to analyze and describe a geometric form tolerance. This model is well suited to *analyze* and *synthesize* profiles across multiple wavelengths or scales. In addition, the fractal representation provides a foundation by which a methodology for functional tolerancing can be developed.

2. The Tolerance–Function Relationship

The inter-relationship between tolerances, or meso-geometric errors, and the functionality of machine elements remains ill defined and poorly understood

[32]. The elucidation of such a relationship is a pressing need in the modern contest of advances in materials and manufacturing technology. New materials and manufacturing techniques pave the road for achieving higher precision in machine components. For example, the Rolls-Royce company predicts a significant increase in gear box capacity for aerospace geared powered transmissions, with a reduction in the gear tooth composite error [15]. The same company also projects improved compressor efficiency, as a consequence of more accurate aerofoil profiles in the rotor and stator blades of axial compressors. While the predicted improvement in performance is promising, the designers do not have the tools to specify, understand, and control the errors on machine elements, in a cost-efficient and effect manner. Closely related problems are comprehension of the dynamics of current and emerging manufacturing processes, and characterizations of their precision. These problems are definitive of the impediments in DFM, and are addressed in this research, with special emphasis on the relation between errors and product function. A design example is presented in this section and developed throughout the paper to illustrate explicitly the influence of manufacturing errors on design performance.

2.1. Functional Tolerancing in a Design Methodology

As motivation for the theory, methodology, and results presented in this paper, consider functional tolerancing in the context of modern engineering design. Figure 1 shows a simple, yet illustrative abstraction of parametric design. The black box contains a functional representation of the design, $f(\ )$. The desired output, or metric, of the design is represented by the performance parameters $\vec{p}$. The decisions that the designer may make are represented by the design parameters $\vec{d}$. Also shown is $\vec{t}$, the tolerance assignments to the design. The space $\vec{t}$ is a subspace of the general design space $\vec{d}$. It is shown here, distinct from $\vec{d}$, because tolerance decisions are the subspace of interest in this study, especially in conjunction with the geometric and material choices $\vec{d}$. Figure 2 is a

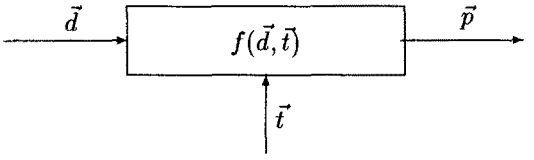

Fig. 1. Tolerance and design parameters affecting performance in the design space.

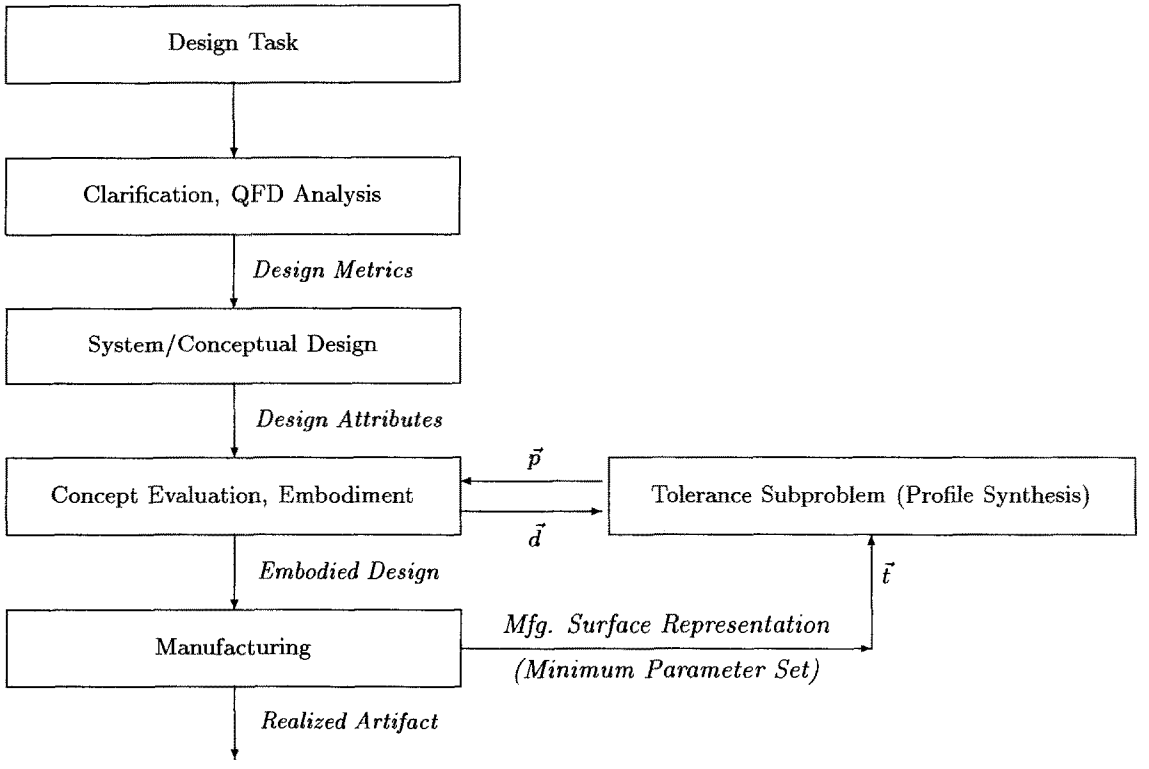

Fig. 2. General steps in a design methodology, including the tolerance sub-problem.

Table 1. Examples of tolerance sub-problems categorized by element interface.

Category	*Tolerance sub-problem*	*Form tolerance of relevance*	*Design metric*
Solid–solid	Gears [15]	Profile	Transmission error Backlash, efficiency, wear, ...
	Piston-cylinder	Circularity	Efficiency, seal force, ...
	Cam-follower [41]	Profile	Vibration Shock, wear, ...
	Press fit bearings [31]	Circularity	Friction, wear, ...
	Ball bearings [29]	Circularity	Vibration Deformation, noise, ...
	Brakes	Flatness, profile	Pressure, force, ...
Solid–liquid	Journal bearings [27, 31]	Circularity	Load carrying capacity Friction, stiffness, damping, ...
	Ball point pen	Profile	Line uniformity Line width, ...
Solid–gas	Air foil	Profile	Lift, drag, noise, Stagnation pressure, ...
	Valve regulator [17]	Roundness, straightness	Flow rate, uniformity, ...
	Computer disc [31]	Profile	Alignment, heat transfer, ...
Solid–light	Optics [37]	Profile	Gloss, focal point, ...

further refinement of the design process. The major components of design are shown, with the tolerance subproblem shown separately for emphasis. A graphical description for the tolerance subproblem is further refined in Sections 3 through 6, as embodied in Fig. 5.

In the context of design metrics representing functionality, the tolerance subproblem is a critical element of the design process in many cases. A range of examples are listed in Table 1, illustrating the categories of physical interfaces that tend to govern the function–tolerance interaction. It is clear from the table that many important tolerance subproblems exist, encompassing a wide range of critical functional issues, such as noise, efficiency, wear, and heat transfer. While the list in Table 1 is not exhaustive, the functional performance of the examples is obviously affected by a form tolerance. Thus, the functional performance of a device may be used to specify geometric tolerances directly, based on a mathematical representation of the design metrics. This relationship between design metrics, the tolerance subproblem, and mathematical representation (Fig. 1) provides our definition for a *functional tolerance*. The examples listed in Table 1 further provide motivation for our work, and illustrate the need to represent manufacturing directly in design through performance metrics. The basic question then becomes how do we abstractly represent manufacturing surface profiles with a minimum set of parameters so that we may incorporate these parameters directly within the design metric relationships (Fig. 2)?

2.2. A Motivating Example

To clarify the general design methodology, an example is used. The example is the design of a lathe head stock (or, in general, an electro-mechanical system). The example presented is not intended to be a complete application of a design methodology but rather to clarify the use of the methodology for functional tolerancing.

The design task is to design a lathe. The lathe is a standard manual feed lathe. A primary customer of the lathe head stock is a machinist or manufacturing firm. Three needs of the customer are accuracy, long-life, and quiet operation. Translating the customer requirements into engineering requirements is, perhaps, the most important step of a QFD analysis. There are many design factors that contribute to the ability of the lathe to produce accurate parts. One major factor in lathe accuracy is how much it vibrates. The engineering requirement for accurate parts can now be cast as minimizing vibration amplitude A and maintaining the vibrations frequency ω above, or below, a certain range.

We now generate a brief functional description of the lathe. In addition to being a necessary step in the design process, the functional description and sub-function solutions show the source of lathe vibrations. A general set of operational functions for the lathe are: (1) provide cutting power, (2) generate cutting motion (rotation), (3) convey cutting motion and power to workpiece, (4) hold and locate workpiece, (5) hold and locate cutting tool, (6) provide

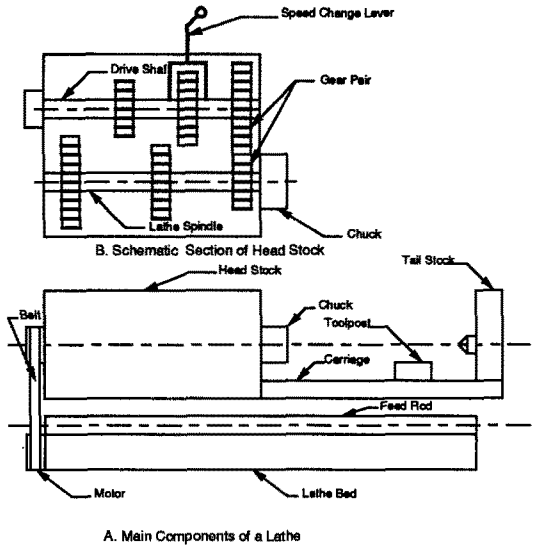

Fig. 3. Schematic of Lathe Head Stock.

relative motion between the tool and the workpiece in two, orthogonal directions, (7) house components, and (8) provide support structure.

For the lathe concept shown in Fig. 3, the motor provides the main motive power. The spindle provides the main cutting motion for the lathe. The cutting power is transmitted from the motor to the spindle using a belt and a set of gear pairs. The chuck attachment to the spindle is used to hold the workpiece. The tool post mounted on the carriage carries the tool and moves the tool perpendicular to the workpiece. Motion parallel to the workpiece is provided by the feed rod. The tail stock is used to support long workpieces and, in addition, to drill longitudinal holes. The head stock houses all the above components. The head stock is constructed on the lathe bed.

Shown in Fig. 3B is a schematic cross section of the head stock. The gear pairs are used to select different speeds for the lathe spindle from the drive shaft connected to the motor by means of a belt drive. The speeds are selected by engaging a different gear pair using the speed change lever. Each pair of meshing gears in the gear box is a source of vibratory excitation. The vibratory energy originating at each gear mesh is conducted to the housing and its supporting structure through the interconnecting structural paths. Gear noise is identified as being the result of force and displacement excitations at the gear mesh which then cause a dynamic response of the shafts and bearings of the transmission system. Forces at the bearings then excite the housing, causing it to vibrate. The head stock houses the spindle and power transmission elements of the lathe. Vibration in the gears affects the accuracy of the machine as well as causing noise in the shop environment. Thus, vibration is an important performance criterion and engineering requirement.

One of the significant factors affecting gear vibration is the geometric errors in the meshing gears. The geometric errors lead to vibration and ultimately translate into workpiece inaccuracies. Another ergonomic effect is the noise caused by the vibration. Relating both of these back to the customer requirements, an engineering need is to reduce transmission error. This brings to focus the tolerance subproblem of design. In order to control the transmission error, the designer must choose, i.e., design, the appropriate tolerance for the gears. Relating back to the QFD analysis, the design metric is now transmission error. The question remains: What is the appropriate form tolerance for the gears and how do we assure that it is achieved?

2.3. Tolerance Subproblem: Gear Transmission

After applying the general design methodology to generate design concepts (Fig. 2) and isolating the important design metrics, a model for the tolerancing subproblem is needed. An articulative tolerance subproblem for the lathe head stock focuses on the relationship between profile errors in gear teeth and transmission error, a parameter of gear noise/vibration. The necessary model is formulated below, and subsequently used to illustrate the functional tolerancing methodology.

Gears are popular machine elements used in rotary power or motion transmissions. Two of the most important design problems confronting a gear designer are the vibration and noise of gears [9]. In addition, monitoring gear noise gives early indications of failure or fatigue [9]. In this example, a parameter called transmission error, which has strong correlations with gear noise, is used as the performance parameter [10].

2.3.1. Definition of Transmission Error

The transmission error is defined as the deviation of the position of the driven gear, relative to the expected position that the driven gear would occupy if both gears were geometrically perfect and undeformed [9]. The two main contributions to the transmission error as inferred from the definition are manufacturing errors in the tooth geometries, and the elastic deformation of the teeth under load [14]. In other words, a gear pair with infinite stiffness and perfectly involute profiles would have zero transmission error [14].

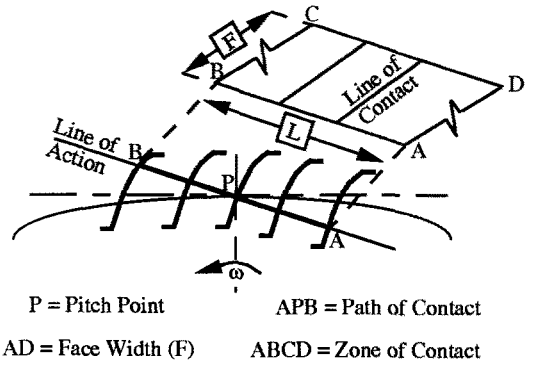

Fig. 4. Contact zone for spur gear pair.

In order to facilitate an assessment of manufacturing errors on performance, the problem is cast as follows. Consider a spur gear pair, with involute teeth. The *path of contact*, the locus of the points of contact (from the beginning to the end of tooth engagement), is defined by a straight line. Since contact takes place across the face width, we can define a rectangular *zone of contact*, with sides defined by the length of contact L, and face width F, as shown in Fig. 4.

The expression for transmission error is given by [10, 14]:

$$TE(x) = \frac{W + \sum_{i=1}^{n} \varepsilon_i(x) k_i(x)}{\sum_{i=1}^{n} k_i(x)} \quad 0 \le x \le L \qquad (1)$$

where W is the load transmitted by the mesh, n is the number of simultaneously meshing tooth pairs in the zone of contact, $\varepsilon_i(x)$ and $k_i(x)$ are the local composite error and the local stiffness of tooth pair i within the zone of contact respectively. The composite error is defined as the sum of the profile errors on meshing teeth at the point of contact, and by definition $\varepsilon_i(x) \ge 0$.

The popular manufacturing processes for gears are hobbing and shaping. Grinding and lapping are finishing processes, used for precision gears. The variations inherent to manufacturing processes have a random component, which cannot be predicted before a gear is manufactured [14]. Hence, a rational basis for relating component errors to performance, without resorting to expensive trials, is required in order to realize the benefits of improved performance. The following sections present such a basis couched in a methodology for the tolerancing problem, within the framework of Design for Manufacturing.

3. Modeling of Machining Errors

As a first step in developing a functional tolerancing methodology, a model is needed of manufactured surface profiles. This model is needed to determine the abstract parameters for the design metrics, and is based on the surface geometry. Surface geometry is a complex imprint of the multitude of physical mechanisms generating the manufactured surface. Straightness is assumed to be the prototypical form error in the following description. A machined surface is assumed to be composed of straight line elements; the variations in the height of the profile are measured as a function of the horizontal coordinate, x, and expressed as $y(x)$. A further practical assumption is that the error values are available in discrete form; i.e., the profile is sampled at N points spaced uniformly along the x axis. Such an assumption is valid and necessary in the example used in this paper as the data is sampled using digital computers. If the sample length is L, i.e., $(0 \le x \le L)$, then the equivalent discretized representation is $(0 \le n \le N-1)$; the errors are expressed as a function of n, and are denoted $y(n)$.

Any model development must be preceded by a decomposition of the profile into mathematically tractable components. Actual machining profiles possess a number of characteristics, e.g., trends, which are loosely interpreted as slopes, periodicities, and so on [36]. A novel representation of a machined profile is to resolve surface profiles into mutually uncorrelated deterministic, and nondeterministic components [21, 26], and investigate the surface based on a superposition model.

There are physical mechanisms associated with each mathematical component. The following sections examine and relate the possible causes of a specific component to the dynamics of the process and/or the error sources, and also prescribe a model representing that component.

3.1. Trend Component

Physically, the slope can be interpreted as a static error, which can be attributed to any one or more of the following causes: error in machine table, error in the fixture, error carried over from a prior process, i.e., roughing, unleveled machine foundation, etc.

We approximate the trend $y_t(x)$ with a straight line, isolated by using linear regression techniques [24]. This procedure compresses the trend information into two parameters, i.e., an intercept y_{t0}, and a slope s_t.

$$y_t(x) = y_{t0} + s_t x \qquad 0 \le x \le L \qquad (2)$$

The linear regression procedure also yields a correlation coefficient, a measure of the significance or 'strength' of the trend component. The absolute value of the correlation coefficient varies between 0 and 1.

3.2. Periodic Component

When the surface profiles exhibit a repetitive pattern, the presence of a periodic component is indicated. We estimate this component from the surface profile by using a nonlinear regression procedure [23, 24]. The following model is used for evaluating the periodic component $y_p(x)$:

$$y_p(x) = y_{p0} + d_a \sin(2\pi f_r x/L) \quad 0 \le x \le L \quad (3)$$

where, y_{p0} is an offset (from an arbitrary datum of zero), d_a is the amplitude, and f_r is the frequency. The discrete counterpart of f_r is referred to as 'frequency number' [26].

3.3. Nondeterministic Component

The nondeterministic components are usually assumed to be independent, identically distributed (i.i.d.) [2] random variates. However, in any typical manufacturing process, there is an intricate interplay of random and (remnant) deterministic effects, leading to spatial interdependence between the errors [26]. A novel approach used in this research is the application of fractal concepts and parameters to model the nondeterministic component in manufactured profiles. The reason for adopting the fractal model stems from the complex interactions of deterministic effects (e.g., vibrations) and random effects (e.g., heterogeneous workpiece hardness) that occur in the course of machining. This complexity engenders a specific structure (e.g., long-term correlations) in the resulting errors, which are elegantly modeled using fractals [26]. The central idea of fractals as applied to surface profiles is examined below.

3.3.1. Fractal Model

Fractals are used for the description of irregular objects, and the main parameter used is the fractal dimension, an effective descriptor for the complexity in a geometric entity [13]. Geometric objects are traditionally described from an Euclidean viewpoint as having (integer) dimensions of 1 (line), 2 (plane), etc. These are 'ideal' geometries, in that there are no errors. Fractal dimensions are non-integer and hence permit the characterization of irregular geometries; the fractional part of the dimension is a measure of the deviation from the ideal geometry. There are several fractal models based on a variety of scaling properties [13]. The model used in this paper is based on the following spectral property of fractal profiles:

$$S(\xi) \propto \xi^{-\beta(D_f)} \quad (4)$$

where ξ is the frequency, and $\beta(D_f)$ is the spectral exponent, a function of the fractal dimension, D_f. This function is model specific; such models can be found in Srinivasan [26].

In the following sections, we describe the mathematical tools used in the identification of the presence of each component, and where applicable, explain the calculation of relevant model parameters. By so doing, we develop the necessary manufacturing representation in Fig. 2.

4. Tools/Models for Detection/Estimation of Form Error

Two techniques are used to test the profile for the presence of deterministic structures. They are: autocorrelation function and power spectrum. The physical interpretations and mathematical definitions of the above quantities are given below, in addition to their nondeterministic counterparts.

4.1. Autocorrelation Function

The autocorrelation function, denoted $\rho(h)$, is a measure of the dependence structure in the profile; i.e., it indicates the degree of similarity between a profile, and a copy of itself, translated by h units (h is referred to as the lag) along the horizontal axis. Equivalently, $\rho(h)$ is interpreted as a measure of the dependence of the profile value at a given location, on the profile value h units downstream.

Recall the profile data is available in discrete form, $y(n)$, $0 \le n \le N-1$; the mathematical expression for the autocorrelation function is obtained in terms of the autovariance function, $\gamma(h)$, estimated as [2]:

$$\gamma(h) = \frac{1}{N-1-h} \sum_{n=0}^{N-1-h} y(n)y(n+h)$$

$$h = 0, 1, 2, \ldots, N/4 \quad (5)$$

The autocorrelation function is then estimated as:

$$\rho(h) = \gamma(h)/\gamma(0) \quad (6)$$

This normalizes the autocorrelation function with respect to unity at zero lag. A plot of $\rho(h)$ as a function of h is referred to as a *correlogram* [2].

Relating this to the deterministic sub-components, the correlogram indicates the presence of a slope, by exhibiting slow decay of $\rho(h)$, as the lag h increases [2]; in contrast, a periodic component in the profile is reflected in a periodic correlogram [2].

4.2. Power Spectrum

The power spectrum is the frequency domain counterpart of the autocorrelation function and is defined as the square of the Fourier Transform (amplitude) per unit length [20]. Such an estimate of the power spectrum is called the *periodogram* [2]. It can be interpreted as a measure of the energy per unit length (or the power) contained in the signal as a function of spatial frequency.

$$S(\xi) = \frac{1}{L}\left|\int_0^L y(x)\, e^{-2\pi i x\xi}\, dx\right|^2 \tag{7}$$

For calculation purposes, the discrete Fourier transform (DFT) [35] of the data is calculated, and then the square of the magnitude is computed to obtain the power spectrum.

The power spectrum reveals the presence of offsets by a peak at zero frequency, and periodic structures by peaks at the underlying frequencies. Hence it can be used to obtain a preliminary estimate of the frequency, before using more rigorous computations to determine the exact parameter values; i.e., the value of the discrete frequency which exhibits a peak in the spectrum is used as an initial estimate for f_r in Eq. (3) in the nonlinear regression.

While the above tools suffice for identifying and quantifying the deterministic components, the fractal parameters describing the nondeterministic component are estimated using the wavelet transform, described in the next section.

4.3. Wavelet-Based Method for Fractal Parameters

The theory of wavelets originated from tools developed for seismic studies. Wavelets share the properties of *statistical self-similarity* and *nonstationarity* with fractals [8]. Hence, given a surface profile, wavelet theory is used as a 'mathematical profiler' to extract the fractal parameters [26]. The essentials of the theory are summarized below.

4.3.1. Profile Analysis with Wavelets

Wavelet analysis yields two sets of information: *approximations* and *details* [4, 12]. An approximation of a profile at a certain scale is defined as the projection of the profile onto the corresponding approximation space. The basis functions of these approximation spaces are built from the dilations and translations of the so-called scaling function. The information lost in stepping from a finer approximation to a coarser one is called the detail, computed by projecting the profile onto the corresponding detail space. The basis functions of the detail space are constructed from the dilations of translations of a wavelet function, which in turn is built from the scaling function. These operations are performed recursively over several scales.

The approximation and detail extraction steps are represented as filtering and sampling operations of the original profile. The corresponding filter coefficients are h_k and g_k respectively. These coefficients embody the characteristics of the corresponding basis functions, and the number of coefficients are directly proportional to the regularity of the functions.

Implementation In the following development, we indicate resolution level by m, and the corresponding scales are dyadic, i.e., 2^m. The output of a profiling instrument is at a specific resolution, depending on the instrument capabilities and the desired measurement scale. This is taken to be the 'base' resolution for the multiresolution analysis and is denoted by $m = 0$. Since the profile is usually given in terms of the height (from a specified datum) at discrete points along the workpiece, this data sequence is indicated by $(A_0^k y)_d$, where d indicates the discrete nature of the data. The approximations and details at resolutions $m < 0$ (find-to-coarse) can be obtained as shown below.

Approximation

$$(A_m^k y)_d = \sum_{n=-\infty}^{\infty} \tilde{h}_{2k-n}(A_{m+1}^n y)_d \tag{8}$$

Detail

$$(D_m^k y)_d = \sum_{n=-\infty}^{\infty} \tilde{g}_{2k-n}(A_{m+1}^n y)_d \tag{9}$$

The reconstruction of the original profile from the approximations and details at various resolutions (coarse-to-fine) can also be computed recursively as:

Reconstruction

$$(A_{m+1}^k y)_d = 2 \sum_{n=-\infty}^{\infty} [h_{k-2n}(A_m^n y)_d + g_{k-2n}(D_m^n y)_d] \tag{10}$$

The three operations presented above, i.e., approximation, detail extraction, and reconstruction can be shown in terms of 'filters' interpretation, as described in Srinivasan [26]. $A_{m+1}\, y$ represents the signal at resolution $m + 1$. This is decomposed into approximation $A_m y$, and detail $D_m y$, by passing it through two filters $\tilde{H}$, and $\tilde{G}$ respectively.

4.3.2. Fractal Profile Synthesis with Wavelets
Fractal profiles and surfaces are characterized by power spectra $S(\xi)$ of the form:

$$S(\xi) \propto \xi^{-\beta(D_f)} \tag{11}$$

where ξ is the frequency and β is the spectral exponent, a function of D_f, the fractal dimension. Wornell [40] presents a scaling argument in terms of the variance of the discrete detail signals $(D_m^k y)_d$:

$$\sigma^2[(D_m^k y)_d] = V_0 2^{-\beta(D_f)m} \tag{12}$$

where V_0 is the magnitude factor. Hence a given surface profile can be decomposed into approximations and details at successively coarser scales. Since the profile information is abstracted in terms of $\beta(D_f)$ and V_0 in Eq. (12), these parameters are calculated from the slope and intercept of the log–log plot of the variance of the details versus the scale 2^m. In addition, discrete details are generated as the samples of a zero-mean Gaussian process, with variance as calculated above. After obtaining the details at all scales, the profile is *synthesized* at successively finer resolutions using Eq. (10).

At this point, the various components of profile structure have been examined, from the causal and mathematical extraction points of view. However, the actual composition of the various components, and their adequacy for a complete description are unclear thus far. These issues are addressed in the next section, leading to a complete model of the manufactured surface.

4.4. A Novel Superposition Approach

The basic superposition model for representing the deterministic and stochastic components of machining errors was discussed earlier. An important assumption in this model is that these components are independent of each other. With the sub-division of the deterministic component into trend and periodicity, the superposition approach is still valid, as discussed below.

An empirical guideline in time series analysis suggests that the periodic component is independent if its amplitude is relatively constant [2]. A review of published error profiles indicates a constant periodic amplitude [36]. Furthermore, the mechanisms causing trend (e.g., static fixture error) and periodicity (e.g., feed) lead to well-defined components, which can be treated as independent of the fractal component. While these three mechanisms would capture the predominant structural information in the profile, it is possible to obtain a few points that do not conform to this overall structure. In statistical parlance, such unrepresentative points are called 'outliers' [1], and for the sake of completeness, they are also added to the model to obtain:

$$y(x) = y_t(x) + y_p(x) + y_f(x) + y_0(x) \tag{13}$$

where $y_0(x)$ is called the outlier component.

This overview of tools and models, comprises one half of the methodology. In the next section, the instructions or steps to use these tools are provided.

5. The Steps in the Methodology

The tools introduced in previous sections for extracting structural information provide a suitable abstraction of manufactured profiles. However, a concerted and cogent procedure for the effective use of these tools is also required to realize truly their potential in DFM. The development of such a methodology would reduce the subjectivity in tolerance assignment, widespread in current industrial practices, and establish a systematic approach for functional tolerancing.

The tolerancing methodology has three main stages, as shown in Fig. 5. The first stage is problem identification, second, error analysis and representation, and third, synthesis and validation. The first and last stages are in the design domain, while the second stage is in the manufacturing domain. The structure of this methodology reflects the interaction between the

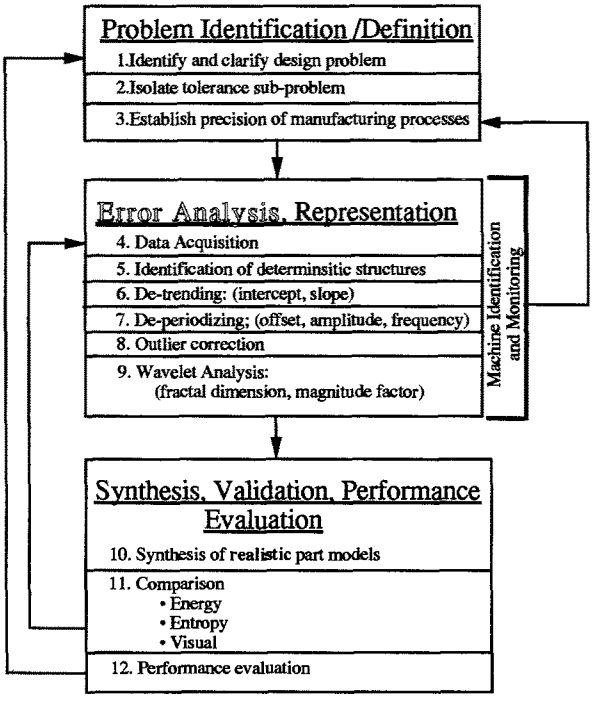

Fig. 5. Steps in proposed tolerancing methodology for DFM.

design and manufacturing domains, required to address the tolerance problem. The three stages are further decomposed into several steps to present the methodology in a logical and evolutionary fashion. Initially, all the steps are presented, without recourse to examples. Then, each step is illustrated with examples.

The following steps comprise the tolerancing methodology in DFM.

1. Identify and clarify design problem: This generic step is mandatory to comprehend the requirements of the customer clearly [19]. For example, this step can involve the decomposition of the overall problem into manageable sub-problems, and identifying conceptual solutions for each. In the example presented in Section 2.2, the sub-problem is power transmission. The customer need is an accurate, long-life, and quiet lathe.
2. Isolate tolerance sub-problem: This step involves a number of nontrivial steps, like determining performance parameters susceptible to surface errors, identifying the appropriate size and geometric tolerances to be prescribed, and establishing the equations governing the inter-relationship. Figures 1 and 2 provide an approach for completing this step, wherein customer needs are transformed into design metrics, that are in turn represented by mathematical models that prescribe the necessary geometric tolerance. In the lathe design example the tolerance sub-problem is the profile tolerance on the gear teeth. The performance parameter (or design metric) is transmission error, given by Eq. (1). Table 1 lists a representative range of tolerance sub-problems.
3. Establish precision of manufacturing processes: At this juncture, the designer must have a knowledge of the precision or the capabilities of the manufacturing processes at his or her disposal. To obtain this knowledge, this phase of the methodology moves into the manufacturing domain. All the different tools described hitherto are called upon to identify, extract and represent the various features. This study is restricted to form errors that can be interpreted as signals in one dimension.
4. Data acquisition: The experimental data, $y(x)$, is obtained. This implies the use of suitable measurement methods. There is no attempt made to distinguish measurement errors from actual profile errors in this paper; it is assumed that the transformations induced by the measurements are negligible, and that the measured values are a true indication of the profile.
5. Identification of Deterministic Structures: The autocorrelation function and the power spectrum are computed. As described above, these provide valuable qualitative information about the presence of deterministic structures, e.g., periodicity, slope, etc. The analyst can also glean some preliminary quantitative estimates for some parameters, e.g., frequency of underlying periodic function. At this point a decision to include or exclude the deterministic features in the model is made, depending on their significance, e.g., correlation coefficient.
6. De-trending: If the autocorrelation and spectrum indicate the presence of a significant trend component, the *slope* and *intercept* parameters (Eq. (2)) are determined by linear regression. The raw profile data are then de-trended to obtain the de-trended profile, $y_{det}(x)$.

$$y_{det}(x) = y(x) - y_t(x) \tag{14}$$

7. De-periodizing: Again the autocorrelation and the spectrum are used as indicators of periodicity on the data. If present, the periodic parameters, *offset*, *amplitude*, and *frequency*, are estimated with a nonlinear regression procedure using Eq. (3). The data are then de-periodized, to obtain the residual, which is the irregular component of the profile.

$$y_r(x) = y_{det}(x) - y_p(x) \tag{15}$$

8. Outlier points: The residual profile data are carefully studied, especially for the presence of a few data points which apparently do not conform to the overall structure; these are the outliers mentioned in Section 4.4. They detract from the quality of the data, but at the same time, they could be symptomatic of some very unusual mechanisms in the machining process, e.g., defects in the grinding wheel, possible measurement errors, etc. However, in the contest of surface models, the outliers pose serious impediments for the following reasons. As motivated in previous sections, wavelet analysis is at the heart of this procedure for detecting long-range correlation in surface errors. However, the detail extraction step is very sensitive to singularities [8]. Consequently the presence of a *few* outliers will inflate the detail values, and influence the subsequent calculation of the detail variances.

   In order to avoid this problem, an outlier correction procedure is adopted, where, if the absolute value of a data point deviates from the mean by more than twice the standard deviation of the entire data set, then the value is replaced by that of its predecessor [1].
9. Wavelet analysis: The wavelet decomposition

(refer to Section 4.3) is used on the corrected residual data to obtain the *fractal dimension* and *magnitude factor*. This is the last step in the error analysis phase of the methodology, and the next step advances into the synthesis and validation stage.

10. Synthesis: In this phase, the designer has the information about the precision of manufacturing processes. The next action is the evaluation of the performance using the governing equations established in Step 3. In this quest, a part model is synthesized using the parameters obtained from the preceding steps.

    The synthesis procedure is a replica of the analysis procedure, but in reverse order. The synthesis of the irregular component uses the wavelet synthesis procedure as described in Section 4.3.2. The generation of the trend and periodic components is trivial, as they follow their respective models (Eqs (2) and (3)). Using these different components, the complete profile is generated by the superposition model, Eq. (13).

11. Comparison: While the synthesis yields *an* error profile, the issue of the 'goodness' of the synthesized profile, with respect to the experimental, warrants some criteria for comparison. The following are used as 'measures' to evaluate the two profiles.

    - Energy: This is intended as a global measure of the *size* of the error, and is defined as [3]:

$$\mathscr{E}(y) = \sum_{n=0}^{N-1} |y(n)|^2 \qquad (16)$$

    - Entropy: This criterion is used as a relative measure of the disorder in the profile; entropy increases with increasing disorder in the profile [6]. An estimate for the entropy is given by [33]:

$$\mathscr{I}(y) = N^{-1} \sum_{n=0}^{N-1} \log\left(\frac{N}{2m} y_{(n+m)} - y_{(n-m)}\right) \qquad (17)$$

      where m is a positive integer smaller than $N/2$, and $y_{(n)}$ are the order statistics[1].

    - Visual Comparison: Any radical differences can be immediately detected by a qualitative visual comparison, even before invoking the quantitative criteria [16]. However, this measure is not a substitute for the other precise, and well-defined criteria, but is only to be used in conjunction with them.

12. Performance: While the above criteria do offer some means of comparison, the true validation of the synthesis would be to evaluate the performance of the part. This falls into the natural framework of the methodology, as this is the next step after synthesis. Hence performance evaluation serves a dual purpose: it acts as an additional criterion for comparing the experimental and synthesized profiles, and also consummates the methodology.

The steps outlined above are explained with reference to a particular example design problem, and a candidate manufacturing process. The design problem is clarified in the next section, including the analysis of machined profiles through an experimental design strategy. The application of the methodology is then revisited to illustrate the utility of the theory for the designer.

6. Implementation of the Methodology

A methodology for the overall design process comprises three stages: conceptual design, embodiment design, and detail design [19]. The methodology for functional tolerancing can theoretically fit into any one of these stages, but it is potentially most useful in the conceptual and embodiment design stages, as shown in Fig. 2. Tolerances have typically been relegated to the final stages of design, since the designer does not possess the knowledge or the tools to represent and manipulate the manufacturing variabilities. These decisions are important at this stage of the design, since an awareness of the tolerances would help direct the choice of resources, e.g., manufacturing processes, in the succeeding stages. The following design example illustrates a design problem, highlighting tolerance selection, using the proposed methodology. The initial phase, comprising steps 1 through 3, is implemented in the following subsections.

6.1. The Design Problem and the Tolerance Sub-Problem

The design problem considered for study is established in Section 2.2. The tolerance problem is the gear transmission. The performance parameter is transmission error, given by Eq. (1).

6.2. Establish Precision: The Gringing Operation

Surface grinding is the manufacturing operation studied (Fig. 6). Here a grinding wheel is mounted on an horizontal spindle, and the workpiece is clamped

[1] Order statistics: If the profile errors are arranged in ascending order, from $y_{(0)}$ the smallest, to $y_{(N-1)}$ the largest, then $y_{(0)}$ is the first order statistic, $y_{(1)}$ is the second order statistic, and so on.

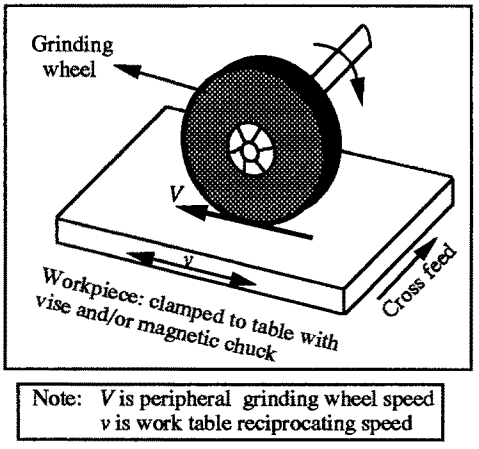

Fig. 6. Surface grinding operation.

on a reciprocating table, typically using a magnetic chuck [11]. A suitable depth of cut is set, and as the table reciprocates beneath the grinding wheel, material is removed by abrasive action. Transverse motion is obtained by cross feed as shown in Fig. 6. The grinding wheel can be considered as an agglomeration of multiple cutting edges, with each abrasive grain acting like a single point tool. However, the geometry of the cutting tools is inconsistent, due to the random orientations of the individual grains. Therefore the grinding process has a predominant random component. Deterministic effects due to vibration are also present [11]. The effects of premature deformation of the workpiece, ahead of the cutting region, are also cited in the same reference. The combination of these numerous error mechanisms produces complex structural effects in the error profiles.

For the experiments in this study, aluminum is chosen as the work material due to its availability and cost. This material is used only for the purpose of illustrating the methodology; the steps would equally apply for steel alloys or exotic gear materials. The grinding experiments are carried out on a Brown and Sharpe 618 Micromaster surface grinding machine. It is desired to conduct the experimental study with multiple combinations of process parameters. Based on previous studies of the grinding operation [5], two parameters are considered, each at two levels; they are the peripheral speed of the wheel (V) and the work table (reciprocating) speed (v). The wheel speed is changed by using different sized grinding wheels, and ranges from 6259 fpm, down to 53.625 fpm. The work table speed ranges from 3500 fpm to 6.094 fpm. The grinding wheel specification is A46HV, which implies a medium grit, medium (hardness) grade, vitrified bond, alumina wheel. Depth of cut is fixed at 0.0005 in. No coolant is used. Each experiment is replicated to gage experimental error. The order of experiments is randomized in each replicate, to reduce the effects of unknown variations [22].

The methodology (steps 4 through 12) is applied to the profiles obtained from the grinding process, and the steps are presented below, for a representative case. Since there are several experimental profiles, the results involving graphical plots, e.g., autocorrelation function, power spectrum, etc., are not presented for all the cases.

6.3. Data Acquisition

The height variations along a linear element of the surface are recorded using the Surfanalyzer 5000 Profiling System.[2] This system has an accurate linear drive, and a sensitive stylus to traverse the surface, and to record the height variations. The horizontal resolution is 0.1 mm, chosen to accommodate the smallest diameter of the probes used for tolerance measurement [38]. The number of data points is $N = 256$, to yield eight levels of resolution in wavelet analysis and synthesis; i.e., where resolution levels are in terms of 2^m, $-8 \leq m \leq -1$. Two different measurements are made for each test piece (errors measured along two different elements on the surface), the first measurement is denoted 'a', and the second 'b'. For example, II.Da implies the first measurement (a) on the fourth test piece (D) of the second replicate (II).

6.4. Identification of Deterministic Structures

The autocorrelation and power spectrum are calculated. These functions, along with the example grinding profile, are shown in Fig. 7. The spectrum indicates the presence of an offset. In addition, the slow decay of the autocorrelation functions leads to the inference of a slope. Almost all grinding profiles indicate these patterns. No indication of periodic structure is apparent for the grinding profiles. This makes intuitive sense, as randomness prevails in ground surfaces [36].

6.5. De-trending

A linear regression analysis is carried out on the profile data. These results are summarized in Table 2. In this case, all grinding profiles have an intercept, and a slope, as can be inferred from the profile plots, and more definitively from the power spectra. Hence, the detrending operation prescribed by Eq. (14) is carried

[2] A product of Federal Products Corporation, Providence, Rhode Island.

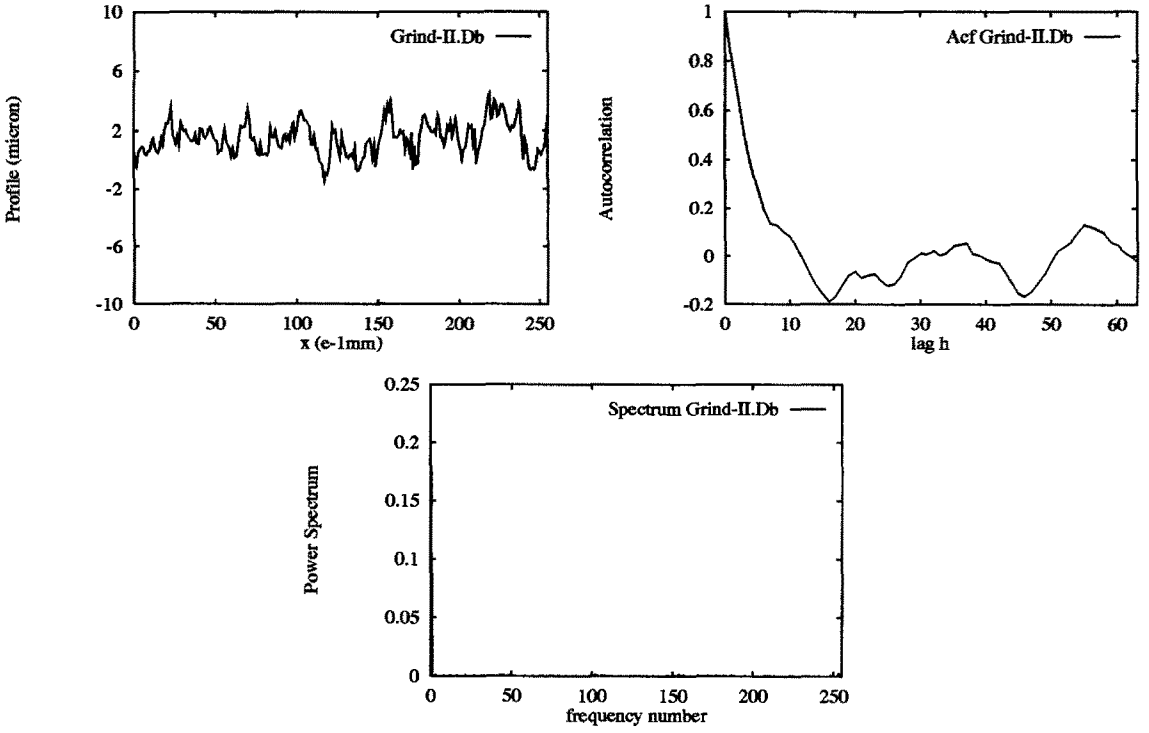

Fig. 7. Grind-II.Db: Profile, autocorrelation function, and power spectrum.

Table 2. Trend parameters for grinding.

REP. No.	*Slope*	*Intercept* (μm)	*Correlation coefficient*
I.Aa	0.012156	1.752679	0.399
I.Ab	0.019312	1.748268	0.473
I.Ba	0.020890	−0.885780	0.677
I.Bb	0.011962	0.713972	0.493
I.Ca	−0.011039	−0.815722	−0.359
I.Cb	−0.022987	−2.522975	−0.698
I.Da	−0.385428	1.496771	−0.842
I.Db	0.011787	0.588932	0.673
II.Aa	−0.003322	−1.894023	−0.146
II.Ab	0.012707	0.121255	0.600
II.Ba	0.023930	0.278721	0.779
II.Bb	−0.019406	1.086330	−0.700
II.Ca	−0.029827	−0.178365	−0.805
II.Cb	0.006601	0.821609	0.276
II.Da	0.009690	−0.045278	0.570
II.Db	0.002408	1.142413	0.158

out for all grinding profiles, irrespective of the correlation coefficient.

6.6. De-periodizing

Since neither the grinding profiles, nor the autocorrelation functions and spectra indicate the presence of periodic structures, and since the offset is accounted for in de-trending, this operation is not carried out for the grinding profiles. In other words, $y_p(x) = 0$ for grinding. The residual is calculated using Eq. (15).

6.7. Outlier Correction

A scatter plot is used in place of the normal residual plot to perceive the outliers clearly. An example scatter plot is shown in Fig. 8. The limits corresponding to twice the standard deviation are also shown as dotted lines. The few points lying outside these limits do not contribute to the overall structure. This is a common feature in all grinding profiles, and therefore the outlier correction is applied. The corrected residuals are used for the estimation of fractal parameters.

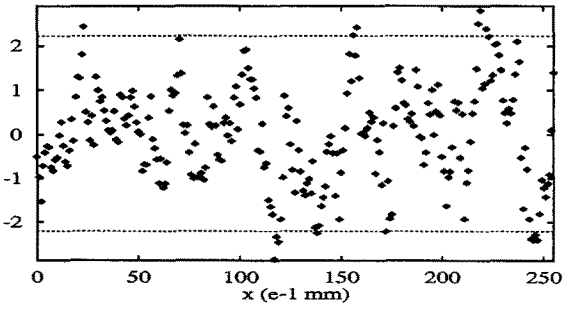

Fig. 8. Plot of typical grinding residual.

6.8. Wavelet Analysis

The wavelet analysis technique is used to calculate the fractal dimension and the magnitude factor. The Daubechies scaling and wavelet functions with twelve coefficients [4] are used in the analysis. The results are presented in Table 3. As the spectral exponent lies in the interval (0, 1), fractional Gaussian noise is used as the underlying model, and the fractal dimension is obtained from $D_f = (3 - \beta)/2$, as explained in Srinivasan [26].

6.9. Synthesis and Comparison

The above parameters (minimal, abstract set) are used to synthesize the corresponding profiles. This step is the link to design, wherein synthesized profiles map manufacturing processes to the design metric models. The example grinding profile, and the synthesized version are shown in Fig. 9. The two are visually similar. The energy and entropy are shown in Table 4. It is clear that the energy and entropy values for grinding experimental and synthesized profiles are in good agreement.

6.10. Discussion of Grinding Profile Parameters

The characteristics of grinding profiles, as exemplified by the fractal parameters, are summarized below.

- These exists a significant trend component in all the profiles. In view of this consistency, the possible cause is the premachining operation. After an initial roughing, the test pieces were moved to a different location for griding, where they were again milled on another milling machine. The presence of trend in all the cases points to a static displacement in the vise, machine table, or foundation of this machine.
- There is no periodic component in any of the grinding profiles. This is expected, as there is no incremental feed leading to periodicities in

Table 3. Fractal parameters for grinding.

REP. No	*Spectral exponent*	*Fractal dimension* D_f^{Δ}	*Magnitude factor* (μm^2)	*Correlation coefficient*
I.Aa	0.456197	1.271902	0.158817	0.697
I.Ab	0.508043	1.245979	0.188157	0.959
I.Ba	0.640279	0.179861	0.103456	0.999
I.Bb	0.425596	1.287216	0.120276	0.983
I.Ca	0.823478	1.088261	0.136429	0.995
I.Cb	0.696449	1.151776	0.110229	0.982
I.Da	0.185799	1.407101	0.062795	0.355
I.Db	0.162700	1.418650	0.065793	0.522
II.Aa	0.464151	1.267925	0.079817	0.794
II.Ab	0.130880	1.143456	0.073059	0.336
II.Ba	0.035566	1.482217	0.239665	0.066
II.Bb	0.102393	1.448804	0.244190	0.309
II.Ca	0.404507	1.252747	0.065129	0.862
II.Cb	0.427942	1.286029	0.067165	0.887
II.Da	0.508013	1.245994	0.030870	0.794
II.Db	0.504878	1.247561	0.057347	0.958

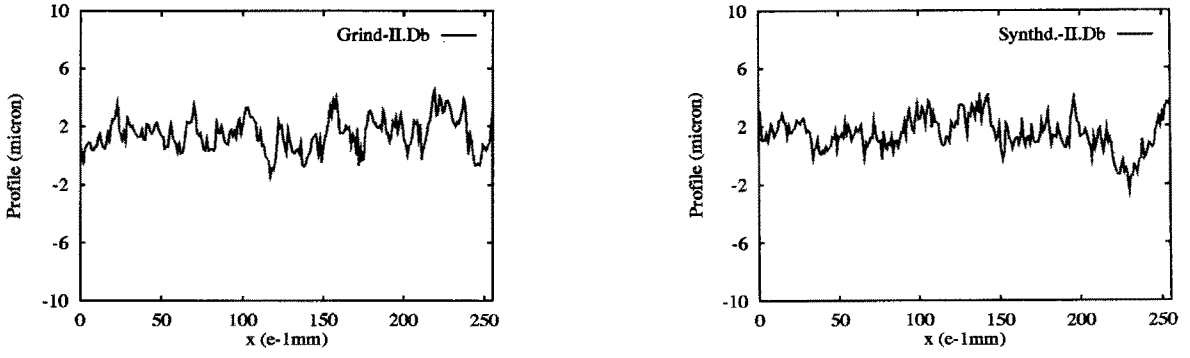

Fig. 9. Experimental and synthesized profiles: Grind-II.Db.

Table 4. Energy and entropy for gringing profiles.

REP. No	*Energy* (mm^2)		*Entropy* (e.u.)	
	Experimental	*Synthesized*	*Experimental*	*Synthesized*
I.Aa	0.004091	0.005233	−4.781622	−4.448349
I.Ab	0.006872	0.008646	−4.465446	−4.206314
I.Ba	0.002140	0.004893	−4.749470	−4.230689
I.Bb	0.002105	0.003103	−4.977645	−4.595289
I.Ca	0.002590	0.004958	−4.769976	−4.296089
I.Cb	0.009132	0.010212	−4.726974	−4.394058
I.Da	0.003304	0.003589	−4.978600	−4.944433
I.Db	0.001549	0.001723	−5.307492	−5.185005
II.Aa	0.002104	0.001901	−5.173342	−5.215548
II.Ab	0.001403	0.001061	−5.126316	−5.498378
II.Ba	0.004159	0.003775	−4.761717	−4.918731
II.Bb	0.001571	0.001697	−4.820007	−4.793002
II.Ca	0.005979	0.006200	−4.695406	−4.558823
II.Cb	0.001506	0.001029	−5.098579	−5.441804
II.Da	0.000767	0.000593	−5.408412	−5.617923
II.Db	0.000862	0.000889	−5.419618	−5.406432

single-pass grinding, in contrast to a process like milling, where the feed gives rise to a periodic component [36].

- The fractal parameters are in the range $1 < D_f^{\Delta} < 1.5$. This indicates low (but still important) irregularity when compared to the ideal dimension of unity. It also implies 'persistence' [13], characteristic of profiles with $D_f^{\Delta} < 1.5$; it means that a positive value in the past will be followed by a positive value in the future. In addition, the fractal model is proved valid for ground profiles in the tolerance scales.

7. Performance Comparison

We now transition from a novel representation of manufacturing processes to incorporating the process representations in design. The performance comparison is presented with the aid of a design example, viz., the lathe gear transmission problem described in Sections 2.2 and 2.3. One of the major sources of gear vibration and noise is transmission error [14], and the relationship between profile errors and transmission is given by Eq. (1). The experimental and synthesized profile data are used in this relationship to investigate their effects on transmission error in the course of meshing.

The parameters for the gear pair used in this study are given in Houser [9]. Using these values, the length of contact L is calculated as [14]:

$$L = \sqrt{R_{tg}^2 - R_{bg}^2} + \sqrt{R_{tp}^2 - R_{bp}^2} - \tan\phi(R_{bg} + R_{bp}) \quad (18)$$

where ϕ is the pressure angle, R_{bg} is the radius of the base circle for the gear, and R_{tp} is the tip circle radius of the pinion, and so on. As the contact ratio is unity, the expression for transmission error becomes:

$$\text{T.E. } (x) = \frac{W + \varepsilon_i(x)k_i(x)}{k_i(x)} \qquad 0 \le x \le L \quad (19)$$

The stiffness values $k(x)$ are calculated by assuming $k(x) = k_0 \cdot x$, where k_0 is a constant stiffness [10].

Grinding profiles are used in this study, specifically the profiles I.Da and I.Db, for one gear pair, and I.Ca and I.Cb for another. First, the experimental data are used as instances of error profiles on a pair of meshing gear teeth (e.g., I.Da as error on driver, I.Db as error on driven). The direct experimental data are superimposed on the gear teeth profiles initially, as opposed to the more abstract and simplified model, for the purpose of verification. Equation (1) is used to calculate 'experimental transmission error', and then the calculation is repeated with the corresponding synthesized errors, to obtain 'synthesized transmission error'. The plots of these errors for one mesh cycle (excluding initial contact) are shown in Fig. 10. Note the similarity in maximum and minimum values, and the overall pattern of the error spectra, verifying the synthesis approach. From the definition of the transmission error, (Eq. (19)), the component due to the compliance, i.e., $W/k_i(x)$, decreases with the progression of meshing [10]. The component due to the profile errors is called the transmission error of 'unloaded gears' [9]. For a perfect gear pair, this component is zero. However, the total transmission

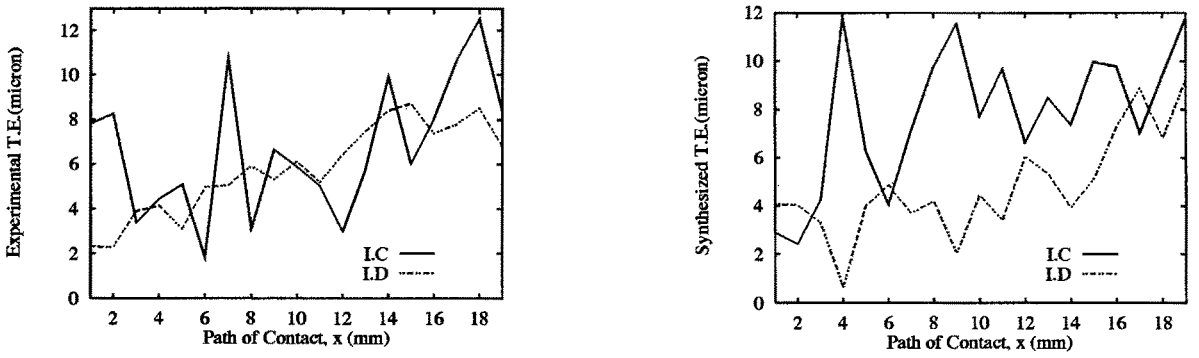

Fig. 10. Transmission error: Experimental and synthesized grinding profiles.

error for both the experimental and synthesized profiles is increasing in a mesh cycle; the magnitude of the error, 10–13 μm, could be acceptable, for example in a concrete mixer. For more critical applications, like machine tool gears for the lathe head stock, this error is unacceptable, indicating the need for more precise gear finishing methods, a different choice of materials, or a change in profile geometry. This result, while being intuitively perceptible, is explicitly derived using a methodological approach. Such an approach provides a rational basis for the designer to address tolerancing problems, e.g., other manufacturing processes and material choices represented by the superposition model may be synthesized and analyzed to determine the process that will satisfy the gear transmission function.

The above example establishes the applicability of the methodology in synthesizing realistic part models. Another benefit that can be derived from this approach is the choice of process parameter combinations that are a compromise between performance and time to manufacture. For example, the designer can compare the performance of the system under various process parameter combinations; i.e., higher speeds and feeds which provide a higher rate of material removal are preferable, provided the performance is acceptable for the application in question. For example, consider the performance of gear pair I.C versus I.D. The former has a larger range of transmission error, which can be attributed to the larger magnitude factor. The significant slope in I.Da also influences the corresponding transmission error. The patterns in the transmission errors reflect to a certain degree, their regularities of the corresponding fractal dimensions. As the magnitude factor dominates the transmission error in this case study, the designer would prefer to choose the parameters of I.D., which also yield the shorter manufacturing time.

8. Conclusions and Future Work

This paper presents a methodology for assigning function-driven tolerances for mechanical components within the framework of DFM. Traditional and novel mathematical tools are used to detect and estimate various structural components in a machined profile. Following a step by step procedure for identifying and characterizing each component (analysis), the profile is synthesized from the parameters. Measures for determining the 'goodness' of the synthesis are also presented. A design example is presented to illustrate the implementation of the methodology, using data from a grinding process. The power of the methodology lies in abstracting the error information in terms of a minimum set of parameters, then used in the synthesis of realistic part models. The use of fractal parameters offers a means for quantifying the structure of the errors, a hitherto unaddressed issue in tolerances.

The current research only addresses one-dimensional form errors. The future challenges lie in extending and/or adapting this methodology to handle two-dimensional form errors and other geometric and size errors. The issues of assemblability also warrant attention. An extension of the experimental component to address other manufacturing processes and parameters is also part of future research.

Acknowledgements

This material is based upon work supported, in part, by The National Science Foundation, Grant No. DDM-9111372, an NSF Presidential Young Investigator Award, and research grants from Ford Motor Company, Texas Instruments, and Desktop Manufacturing Inc. Any opinions, findings, conclusions or recommendations expressed in this publication are

those of the authors and do not necessarily reflect the views of the sponsors. The authors thank Dr Richard H. Crawford of the Mechanical Engineering Department at UT Austin, for his review and critique of the methodology.

References

1. V. Barnett and T. Lewis. *Outliers in Statistical Data.* John Wiley & Sons, New York, 1978.
2. J. S. Bendat and A. G. Piersol. *Measurement and Analysis of Random Data.* John Wiley & Sons, Inc., New York, 1966.
3. J. A. Cadzow. *Foundations of Digital Signal Processing and Data Analysis.* Macmillan Publishing Company, New York, 1987.
4. I. Daubechies. Orthonormal basis of compactly supported wavelets. *Communications on Pure and Applied Mathematics,* XLI(7):909–996, October 1988.
5. D. A. Farmer, J. N. Brecker, and M. C. Shaw. Study of the finish produced in surface grinding: Part 1—Experimental. *Proceedings of the Institution of Mechanical Engineers,* 182:171–179, 1967.
6. J. B. Fenn. *Engines, Energy, and Entropy.* W. H. Freeman and Company, San Francisco, 1982.
7. S. Finger and J. R. Dixon. A review of research in mechanical design. Part ii: Representations, analysis and design for the life cycle. *Research in Engineering Design,* 1(2):121–137, 1989.
8. P. Flandrin. Wavelet analysis and synthesis of fractional brownian motion. *IEEE Transactions on Information Tneory,* 38(2):910–917, March 1992.
9. D. R. Houser. Gear noise sources and their prediction using mathematical models. In *Gear Design, Manufacturing and Inspection Manual,* chapter 16, pages 213–222. SAE, Warrendale, PA, 1990.
10. A. Kubo, T. Kuboki, and T. Nonaka. Estimation of transmission error of cylindrical involute gears by tooth contact pattern. *ISME International Journal,* 34(2):252–259, 1991.
11. S. Malkin. *Grinding Technology.* Ellis Horwood Limited, Chichester, 1989.
12. S. G. Mallat. A theory for multiresolution signal decomposition: The wavelet representation. *IEEE Transactions on Pattern Analysis and Machine Intelligence,* 11(7):674–693, July 1989.
13. B. B. Mandelbrot. *The Fractal Geometry of Nature.* W. H. Freeman and Co., San Francisco, 2nd edition, 1983.
14. W. D. Mark. Analysis of the vibratory excitation of gear systems: Basic theory. *Journal of the Acoustical Society of America,* 63(5):1409–1430, May 1978.
15. P. McKeown. The role of precision engineeering in manufacturing of the future. *Annals of the CIRP,* 36(2):495–501, 1987.
16. B. Melamed. An overview of the tes process and modeling methodology. Technical Report of NEC USA, Inc., 1993.
17. Mikron Corp Monroe. Valve regulator. Monroe, CT.
18. R. F. O'Connor and T. A. Spedding. The use of a complete surface profile description to investigate the cause and effect of surface features. *International Journal of Machine Tools and Manufacture,* 32(1/2):147–154, February 1992.
19. G. Pahl and W. Beitz. *Engineering Design.* The Design Council, Springer-Verlag, New York, 1988.
20. H. O. Peitgen and D. Saupe. *The Science of Fractal Images.* Springer Verlag, New York, 1988.
21. M. B. Priestley. *Spectral Analysis and Time Series: Multivariate Series Prediction and Control,* volume 2. Academic Press, London, 1981.
22. T. H. Chang, R. E. DeVor, and J. W. Sutherland. *Statistical Quality Design and Control.* Macmillan Publishing Co., New York, 1992.
23. SAS Institute Inc., Cary, NC. *SAS/STAT User's Guide, Volume 1 and 2,* fourth edition, 1990. Version 6.
24. A. Sen and M. Srivastava. *Regression Analysis: Theory, Methods, and Applications.* Springer-Verlag, New York, 1990.
25. M. S. Shunmugam. Criteria for computer-aided form evaluation. *ASME Transactions Journal of Engineering for Industry,* 113:233–238, May 1991.
26. R. S. Srinivasan. *A Theoretal Framework for Functional Form Tolerances in Design for Manufacturing.* PhD thesis, The University of Texas, Austin, TX, May 1994.
27. R. S. Srinivasan and K. L. Wood. Fractal-based geometric tolerancing in mechanical design. In *Proceedings of the 1992 ASME DTM Conference,* pages 107–115, Phoenix, AZ, September 1992. ASME.
28. R. S. Srinivasan and K. L. Wood. Geometric tolerancing in mechanical design using fractal-based parameters. *ASME Journal of Mechanical Design,* 117(1): 203–205, 1995.
29. R. S. Srinivasan and K. L. Wood. Wavelet transforms in factal-based form tolerancing. In *1993 Design Theory and Methodology Conference,* pages 51–63, New York, September 1993. ASME.
30. V. Srinivasan, editor. *1993 International Forum on Dimensional Tolerancing and Metrology,* Dearborn, MI, June 1993. ASME.
31. A. Tabenkin. Understanding surface finish. Technical report, Federal Products Corporation, Providence, RI, 1990.
32. V. A. Tipnis, editor. *Tolerance and Deviation Information.* New York, 1992. ASME. CRTD-15-1.
33. O. Vasicek. A test for normality based on sample entropy. *Journal of the Royal Statistical Society,* 38:54–59, 1976.
34. H. B. Voelcker. A current perspective on tolerancing and metrology. *Manufacturing Review,* 6(4):258–268, December 1993.
35. H. J. Weaver. *Applications of Discrete and Continuous Fourier Analysis.* John Wiley & Sons, New York, 1983.
36. D. J. Whitehouse. Surfaces—a link between manufacture and design. *Proceedings of the Institution of Mechanical Engineers,* 192:179–188, June 1978.
37. D. J. Whitehouse. A philosophy of linking manufacture to function—an example in optics. *Proceedings of the Institution of Mechanical Engineers,* 207(B1):31–42, 1993.
38. C. Wick, editor. *Measurement of Circularity,* volume IV of *Tool of Manufacturing Engineers Handbook,* chapter 4, pages 4.27–4.32. Society of Manufacturing Engineers, Dearborn, Michigan, 4th edition, 1987.
39. K. L. Wood, R. S. Srinivasan, I. Y. Tumer, and R. Cavin. Fractal-based tolerancing: Theory, dynamic process modeling, test bed development, and experiments. In *Proceedings of the 1993 NSF Design and Manufacturing Systems Conference,* pages 731–740, Charlotte, NC, January 1993. NSF, SME.
40. G. W. Wornell. Synthesis, analysis, and processing of fractal signals. Technical Report 566, Massachusetts Institute of Technology, Cambridge, MA, October 1991.
41. C. Zhang and H. P. Wang. Tolerance analysis and synthesis for cam mechanisms. *International Journal of Production Research,* 31(5):1229–1245, 1993.